Rhes Deletion Prevents Age-Dependent Selective Motor Deficits and Reduces Phosphorylation of S6K in Huntington Disease Hdh150Q(CAG) Knock-In Mice.

Jennifer Hernandez[#1], Neelam Shahani[#1], Supriya Swarnkar[1$], and Srinivasa Subramaniam[1 *]

[1]The Scripps Research Institute, Department of Neuroscience, Jupiter, FL 33458, USA

[#] These authors contributed equally.

[$]current address: The Jackson laboratory, *in-vivo* Services, Bar Harbor, Maine, 04609, USA. *Correspondence ssubrama@scripps.edu

Abstract

Huntington disease (HD) is a neurodegenerative disease caused by a CAG trinucleotide repeat expansion in the huntingtin (mHTT) protein. This expansion is thought to promote striatal atrophy by a combination of cell- and non-cell-autonomous processes, but the mechanisms are unclear. Previous evidence suggests that the striatal-enriched SUMO E3-like protein Rhes could play a pathological role in HD. Rhes interacts with, and SUMOylates, mHTT and promotes toxicity and Rhes deletion ameliorates the HD phenotype in cell and severe mouse models of HD. However, the effect of Rhes on less severe knock-in models of HD remains obscure. Here, we report that a Hdh(CAG)150 knock-in murine model of HD showed diminished body weight but no changes in locomotor coordination or activity at 80 and 100 weeks of age. Conversely, Rhes deletion did not impact the body weight or behaviors but caused a significant reduction of gait, clasping, and tremor behaviors in $Hdh^{150Q/150Q}$ mice. Rhes deletion did not affect the loss of striatal DARPP-32 protein levels but abrogated the hyper ribosomal protein S6 kinase beta-1 (S6K) phosphorylation, which is a substrate for a mechanistic target of rapamycin complex 1 (mTORC1) signaling, in Hdh(CAG)150 mice. Interestingly, striatal Rhes protein levels were downregulated in the striatum of Hdh(CAG)150 mice, indicating a potential compensatory mechanisms at work. Thus, Rhes deletion prevents age-dependent behavioral deficits and diminishes hyperactive mTORC1-S6K signaling in Hdh(CAG)150 knock-in mice HD striatum.

Key words

Striatal vulnerability, delayed onset, age-dependent, pathology, mild-to-moderate, kinase.

Introduction

Wild-type huntingtin (wtHTT) is a ubiquitously expressed protein with a polyglutamine tract encoded by the *HTT* CAG repeat expansion (mHTT) that causes Huntington Disease (HD). HD is characterized by the early loss of medium spiny neurons (MSNs) in the striatum, and this loss subsequently affects motor and cognitive functions[1, 2]. As HD progresses, it affects other parts of the brain, as well as the peripheral tissues[3, 4]. The mHTT protein and its proteolytically cleaved fragments affect several cell functions, such as vesicle- and microtubule-associated protein/organelle transport, calcium dysregulation, transcription, autophagy, and sphingosine and cysteine metabolism, as well as having effects on tissue maintenance, secretory pathways, and cell division[5-22]. However, the mechanisms underlying HD pathogenesis remain unclear, and the currently available drugs, although providing symptomatic relief, neither prevent nor slow HD progression. Elucidating the mechanism governing striatal abnormalities should therefore provide opportunities for the development of novel and effective therapeutic interventions.

One possible target for these interventions is Rhes, which is highly expressed in the dopamine 1 receptor (D1R), D2R MSNs, and cholinergic interneurons in the striatum[23, 24]. It is also expressed to some extent in other brain regions, such as the cortex and hippocampus[23, 25, 26]. Rhes expression is induced by thyroid hormones, and Rhes can inhibit the cAMP/PKA pathway and N-type Ca^{2+} channels (Cav 2.2)[24, 27-29]. We have found several new roles for Rhes in the striatum; for example, Rhes can bind directly to and activate mTOR in a GTP-dependent manner, thereby promoting L-DOPA-induced dyskinesia (LID) in a pre-clinical model of Parkinson's disease,[30] in agreement with a recent report[31]. We also found that Rhes harbors a C-terminal SUMO E3-like domain and physiologically regulates SUMO modification via the cross-SUMOylation of the E1 (Aos1) and E2 (Ubc9) enzymes[32]. We recently identified several novel nuclear SUMO substrates of Rhes and a role for Rhes in gene regulation[33].

We have demonstrated that Rhes-SUMO signaling plays major roles in HD. For example, we found that Rhes interacts with mHTT and promotes cellular toxicity by

increasing the soluble forms of mHTT via SUMO1 modification[34], in agreement with an independent study[35]. The toxicity of Rhes expression in HD has also been independently demonstrated in various cell and hESC-derived models of HD[36-40], but the underlying molecular mechanisms of Rhes-mediated toxicity remain unclear. Interestingly, Rhes promotes tau toxicity by regulating lysosomal activity and SUMOylation in Tg4510 tauopathy mouse[41], and altered localization and clearance of neuronal Rhes is considered as a novel hallmark of tauopathies[42]. Serendipitously, we found that Rhes can be robustly transported between cells and that it functions as a critical determinant of mHTT transport between neuronal cells via the tunneling nanotube-like (TNT-like) "Rhes tunnel" protrusion[43, 44]. The mHTT cargoes travel through this protrusion and along the membrane of acceptor cells before being internalized[43]. By contrast, SUMOylation-defective mHTT is transported much less efficiently, indicating the importance of SUMO in Rhes-mediated mHTT transport[43]. These results indicate that Rhes–SUMO signaling participates in HD pathogenesis.

Consistent with the above studies, we found that Rhes deletion ameliorated HD pathogenesis in a number of different transgenic (Tg) HD models. Rhes deletion had a marked effect on preventing motor phenotype in male, but not in female, N171-82Q HD Tg model mice[45]. *Rhes*$^{-/-}$ also exhibits a gender effect on dopaminergic-drug induced motor behaviors[24]. A previous independent study showed that Rhes deletion in R6/2, a more severe HD model, also prevented HD-associated motor deficits[46]. However, we found that Rhes overexpression worsened the HD-related motor deficits accompanied by enhanced soluble forms of mHTT in the striatum of 6-month-old *Hdh*$^{150Q/150Q}$ knock-in (KI) mice, which express full-length mutant huntingtin with slowly developing and less severe behavioral phenotype mouse[47] [48], and in the cerebellum of N171-82Q mice[45, 48]. A recent study showed that HAP1 deficiency increases the binding of Rhes to soluble N-terminal mutant HTT and to SUMOylated N-terminal HTT, while promoting selective neuronal loss in the striatum of full-length mutant HTT KI (140CAG) mice[49]. These multiple independent results[34-40, 45, 46, 49, 50] indicate that Rhes plays a major role in striatal neuronal loss by interacting with and modifying mHTT and that its role is modulated by additional proteins in the striatum.

By contrast, microRNA-based depletion of *Rhes* mRNA in the striatum of N171-82Q showed no protective effect. Instead, its depletion in 12-month-old BACHD mice (similar to N171-82Q;*Rhes*$^{-/-}$)[24] resulted in displays of mild hypoactivity, as well as a ~4% decrease in striatal volume as measured by MRI[51]. Overexpression of AAV-Rhes in the striatum of N171-82Q mice improved their rotarod performance[52]; however, in that study[52], Rhes was flag-tagged at the C-terminal end and this could have affected farnesylation and mislocalized Rhes to the nucleus[34]. Nevertheless, these results indicated that Rhes-mediated HD pathogenesis in mice in vivo depends on the choice of HD mouse model, as each may invoke as yet unknown compensatory mechanisms to modify the Rhes-mediated mHTT toxicity. However, the role of Rhes deletion in modulating HD pathogenesis in less severe and late-onset knock-in HD mouse models remains obscure.

Hyperactive mTORC1 is observed in HD by independent studies[53-55], but its role in influencing HD remains controversial. For example, while rapamycin prevented HD phenotype[55], the overexpression of Rheb, an activator of mTORC1, improved HD-like symptoms in mice[52]. In contrast, Rheb overexpression in Drosophila worsened HD-like phenotype[56]. We found depleting TSC1 exacerbated mTORC1 in the striatum and worsened HD-like phenotype in mice[55]. Thus, mTORC1 differentially affects HD, depending upon HD models and assays used to interpret the phenotype. In addition, mTORC1 activation, a key metabolic hub that is controlled by various upstream stimuli may be regulated by mHTT in cell/tissue-dependent manner.

In the present study, we further examined the in vivo role of Rhes on late-onset HD using a Hdh150Q(CAG) KI mouse model[47, 48]. We crossed Rhes-KO with Hdh150Q(CAG) KI mice and carried out the motor deficit and biochemical parameter studies in both male and female mice.

Results

Behavioral assessment of Rhes deletion in Hdh^{150Q} knock-in mice at 80 weeks.

Constitutive depletion of Rhes (Rhes-KO) in the Tg HD R6/2[46] and N171-82Q [45] mice prevented HD-related behavioral and pathological changes. However, the effect of a Rhes-KO in knock-in HD mouse models remains unknown. To test this question, we

crossed Rhes-KO mice with Hdh150Q(CAG) KI and generated Rhes deleted *Hdh*$^{150Q/150Q}$ homozygous and *Hdh*$^{150Q/+}$ heterozygous mice, which developed a late-onset age-dependent HD, with subtle but significant motor abnormalities appearing between 70 and 100 weeks of age[47, 48]. The number of animals (mixed sex ratio) used is indicated in Table 1.

At 80 weeks, no significant effect was observed on body weight in the *Hdh*$^{150Q/+}$ mouse groups compared to the control groups (Fig. 1A), consistent with previous reports[47, 57, 58]. The *Hdh*$^{150Q/150Q}$ mice (n = 10; 3 male) showed a significant loss of body weight, consistent with a previous report[47]. This weight loss was similar to that seen in *Rhes*$^{-/-}$;*Hdh*$^{150Q/150Q}$ (n = 10; 5 male) mice compared to WT (n = 9; 4 male) and *Rhes*$^{-/-}$ mice (n = 12; 5 male, Fig. 1A).

The rotarod behavior tests conducted at 80 weeks in *Hdh*$^{150Q/+}$ or *Hdh*$^{150Q/150Q}$ mice did not reveal any significant defect in the locomotor coordination, and the performance in three different trials was comparable to that of the WT, *Rhes*$^{-/-}$;*Hdh*$^{150Q/+}$ or *Rhes*$^{-/-}$;*Hdh*$^{150Q/150Q}$ groups (Fig. 1B), again consistent with previous studies[47, 58]. Two-way ANOVA of the three trials for each animal revealed no significant difference between the genotypes [F (2, 78) = 2.067, P=0.1334] or interactions [F (4, 78) = 0.06588. P = 0.9919].

Open field tests conducted at 80 weeks in the *Hdh*$^{150Q/150Q}$ mice showed a decreasing trend in spontaneous locomotion in the *Hdh*$^{150Q/150Q}$ mice, and a significant correlation was found between genotypes (F (2, 78) = 4.202, P = 0.0185), but not with the interactions (F (4, 78) = 0.1368, P = 0.9682) or time (F (2, 78) = 1.18, P = 0.3127).

Similarly, behavioral battery tests (ledge, clasping, gait, kyphosis, and tremor) conducted at 80 weeks revealed a significant genotype effect (F (2, 130) = 6.466, P=0.0021), but no significant interaction (F (8, 130) = 1.665, P=0.1128) or time (F (4, 130) = 0.7863). The *Hdh*$^{150Q/150Q}$ mice and showed a trend toward significant defects in the ledge (P = 0.0595) and gait tests (P = 0.0595), and the *Rhes*$^{-/-}$;*Hdh*$^{150Q/150Q}$ showed significant defects in gait compared to WT (P = 0.0011).

Behavioral assessment of Rhes deletion in Hdh^{150Q} *knock-in mice at 100 weeks.*

By the age of 100 weeks, some mice (both male and female) died during the study in all groups: four out of nine (4/9) in the WT, 4/10 in the HD-homo, 3/12 in the Rhes-KO, 3/12 in the Rhes-KO;HD, 2/14 in the Rhes-KO;HD-het, and 7/19 in the HD-het groups.

Body weight remained lower for the *Hdh*$^{150Q/150Q}$ mice but not in the *Hdh*$^{150Q/+}$ groups, while Rhes deletion had no impact on body weight (Fig. 1E).

Rotarod tests showed no significant defects, even at 100 weeks between groups (Fig. 1F), even though previous studies had showed a slight deficiency in rotarod performance around this age in *Hdh*$^{150Q/150Q}$ mice[47, 58]. The difference could reflect the different methodological parameters used. In the original study, no training was used, and the test was conducted at a fixed low-speed setting or with the accelerating rod method run for a maximum of 5 min. In the present case, at both 80 and 100 weeks, we performed the rotarod test using a linearly accelerating rotation paradigm in three trials separated by 20 min for four consecutive days, as described in our previous work[55].

The open field test results showed a significant correlation between genotypes ($F(2, 45) = 4.644$, $P = 0.0147$) but no difference in the interaction ($F(4, 45) = 0.511$, $P = 0.7279$) or time ($F(2, 45) = 0.7255$, $P = 0.4897$) (Fig. 1G).

In the behavioral battery tests, the *Hdh*$^{150Q/150Q}$ mice showed severe deficits in the ledge ($P<0.0001$), clasping ($P<0.0388$), gait ($P < 0.0388$), and tremor ($P <0.0012$) tests when compared to WT mice. Interestingly, the *Rhes*$^{-/-}$;*Hdh*$^{150Q/150Q}$ mice showed significantly decreased levels of ledge ($P < 0.0266$), clasping ($P <0.0266$), and tremor ($P <0.0478$) defects (Fig. 1H).

Altogether, the behavioral data indicated that *Hdh*$^{150Q/150Q}$ mice exhibited late-onset but subtle motor deficits and that Rhes deletion had a significant rescue effect on selected neurological abnormalities at 100 weeks.

Biochemical assessment of Rhes deletion in Hdh^{150Q} *mice.* After the behavioral tests, the heterozygous (*Hdh*$^{150Q/+}$, Fig. 2) and homozygous mice (*Hdh*$^{150Q/150Q}$, Fig. 3) were sacrificed, and their brains were removed for western blot analysis. We found decreased expression of DARPP-32, a striatal neuron marker, in *Hdh*$^{150Q/+}$ and Rhes deletion did not impact DARPP-32 levels in *Rhes*$^{-/-}$;*Hdh*$^{150Q/+}$ (Fig. 2A, B).

We previously showed that mHTT could elicit mTORC1 signaling in the HD cell model[55], so we evaluated mTORC1 signaling in HD mice. We found that striatal mTORC1 signaling targets the phosphorylation of S6K (Thr389) or phosphorylated 4E-BP1 (Ser65) was not significantly upregulated in the striatum in *Hdh*$^{150Q/+}$ mice (Fig. 2A, C).

Autophagy and inflammatory process are also altered in HD[59, 60]. So, we evaluated p62 and LC3BII (markers of autophagy) and GFAP (glial marker) and found no significant alteration of these markers in *Hdh*$^{150Q/+}$ mice striatum by western blotting (Fig. 2A, D).

Interestingly, we found significant reductions in the Rhes levels, but not Rheb, another member of small GTPase[61], in the *Hdh*$^{150Q/+}$ mouse striatum (Fig. 2E).

In homozygous mice (*Hdh*$^{150Q/150Q}$), the DARPP-32 levels were further strongly diminished in the striatum and Rhes deletion had no impact in *Rhes*$^{-/-}$;*Hdh*$^{150Q/150Q}$ mice (Fig. 3A, B).

The hyperphosphorylation of S6K (Thr389) was observed in the striatum of homozygous HD mice. Rhes deletion completely abolished this without affecting the basal pS6K, indicating that Rhes may promote mTORC1 signaling in the striatum under pathological conditions, consistent with previous work[30, 31]. Phosphorylated 4E-BP1 (Ser65), which in some instances can be mTORC1-independent[62], however, is not significantly altered in the striatum of *Hdh*$^{150Q/150Q}$ mice (Fig. 3A, B). Thus mTORC1–S6K pathway is particularly regulated by Rhes in *Hdh*$^{150Q/150Q}$ mice.

Investigation into the autophagy regulators revealed while p62 levels show a trend of an enhancement, but the steady-state levels of LC3BII are unaltered in *Hdh*$^{150Q/150Q}$ mice. Rhes deletion has no impact on p62 or LC3BII levels in *Rhes*$^{-/-}$; *Hdh*$^{150Q/150Q}$ mice (Fig. 3A, D).

Similar to heterozygous *Hdh*$^{150Q/+}$ mouse striatum, a further dramatic reduction of Rhes in the *Hdh*$^{150Q/150Q}$ homozygous HD KI striatum was observed, while the Rheb levels remain unaltered. (Figs. 3A, E).

Altogether, the biochemical results indicated that DARPP32 levels are diminished in *Hdh*$^{150Q/+}$ and *Hdh*$^{150Q/150Q}$ mice. Subtle upregulation of p62 was observed in *Hdh*$^{150Q/150Q}$. Rhes deletion has no impact on DARPP-32 or p62 levels. Rhes deletion, however, diminishes hyperactive mTORC1 signaling in *Hdh*$^{150Q/150Q}$. Finally, Rhes levels are also downregulated in the striatum of HD mice in an mHTT-copy dependent manner.

Discussion

This study reports that global Rhes deletion in a knock-in (KI) HD model provides mild benefits on selected behaviors.

The development of animal models mimicking the human HD remains a significant challenge. Transgenic (Tg) mice models that express a shorter fragment of mHTT (82 to 125 CAG repeats) show the rapid onset of motor symptoms, neuronal death, and premature demise[63-66]. In contrast, knock-in (KI) mice models with insertion of mHTT into exon 1 with superlong expansions (>150Q) develop slow progression, mild symptoms, or no observable HD-like symptoms[67, 68]. In humans, the adult-onset HD comprises >36 CAG, while the juvenile-onset >60 CAGs. The mechanisms for the paradoxical effect– while a human with >60 CAG develops severe disease and premature death while these phenotypes are absent in mouse with >150Q– remain unclear. However, the differences in the mHTT load and mHTT toxic species may determine the onset and the severity of the disease between humans and KI mice. For example, in the KI mouse models, the proteolytic mechanisms that generate toxic forms of mHTT may be suboptimal, or the KI models may have developed compensatory mechanisms that may prevent the severity of the disease.

Previous results indicate that Rhes deletion affords protections from behavioral and pathological deficits in Tg (N171-82Q and R6/2) HD animals[45, 46]. Here we found Rhes deletion in a milder HD model, Hdh^{150Q} KI mice[47, 58], afforded only mild protection (Fig. 1). We found that DARPP-32, a commonly used striatal marker for striatal abnormalities, is diminished in Hdh150Q KI mice striatum (Fig. 2, 3), but these mice do not display any significant motor coordination deficits (Fig. 1). Therefore, it appears that loss of DARPP-32 is not directly linked to behavioral deficits in Hdh150Q KI mice.

Interestingly, we observed that Rhes is also diminished in the striatum of KI mice (Fig. 2, 3). The possibility that downregulation of Rhes in the KI mice may prevents the severity of HD-like symptoms cannot be ruled out. Because when Rhes is replenished in the striatum of *Rhes*$^{-/-}$*;Hdh*$^{150Q/150Q}$ mice, it elicited rapid motor coordination deficits[45]. Therefore, the downregulation of Rhes in KI striatum most likely a protective response. Nevertheless, Rhes deletion afforded protection against specific tests such as ledge, clasping, and tremor (observed at 100 weeks) (Fig. 1) as well as hyperactivation of

mTORC1 signaling in *Rhes*$^{-/-}$*;Hdh*$^{150Q/150Q}$ (Fig. 3). Thus, residual Rhes in the striatum may still promote abnormalities in HD mice.

The mechanisms by which Rhes promotes neurodegeneration are also evolving. Rhes associates with mHTT and induces its SUMO modification, which leads to enhanced soluble forms of the mHTT[50, 69]. The downstream pathology may occur via more than one route. Particularly Rhes-mediated cell-to-cell transport of mHTT, which is partly SUMO-dependent, through tunneling-like nanotubes or cytoneme-like structures may elicit non-cell-autonomous toxicity[43, 70].

Multiple lines of evidence link Rhes in the autophagy regulation. Rhes can activate Akt/mTORC1 signaling to inhibit autophagy[30, 31, 71]. Rhes binds to Beclin1 and promotes autophagy independent of mTORC1[72]. Rhes binds to Nix and promotes selective autophagy (mitophagy)[44]. Moreover, we showed that SUMO regulates mTORC1 and autophagy signaling and prevents HD-related deficits in Q175DN-KI model that show enhanced mTORC1 activity[54, 73, 74]. Previous pharmacological studies with mTORC1 inhibition showed beneficial effects in HD models[54, 75]. Thus Rhes-SUMO may orchestrate HD pathogenesis via mHTT transport as well as mTORC1/autophagy signaling.

Besides HD, Rhes is also implicated in Tau toxicity. Pathogenic tau (*MAPT)* mutations diminished Rhes expression in the hiPSC-derived neurons, and depletion of Rhes attenuated behavioral and inflammatory abnormalities in rTg4510 mice via lysosomal activation mechanism[41]. Histopathology evaluation of tauopathies revealed Rhes is mislocalized or diminished in the presence of abnormal tau in the entorhinal cortex, hippocampus, and superior frontal gyrus. Such specific altered neuronal distribution of Rhes is considered as a novel hallmark of all tauopathies[42]. Thus, alteration of Rhes localization and expression may be a common feature in neurodegenerative diseases.

In summary, our data indicate that global Rhes deletion in a less severe Hdh150Q KI model prevents only selected behavioral and biochemical deficits. Although cellular models and preclinical models could help identify new therapeutic targets, there is a growing difficulty translating these findings to humans. Recent failures of clinical trials in neurodegenerative diseases[76], including HTT ASOs in HD, indicate incompatibility of

murine models with clinical outcomes. Because multiple cellular and preclinical models link Rhes to both mHTT and tau toxicity, the Rhes-targeted therapy is a valuable option. Whether such treatment will diminish neuronal toxicity and increase survival can only be appreciated after the clinical trials and positive therapeutic outcomes.

Materials and Methods

Reagents and Antibodies.

All reagents were purchased from Millipore-Sigma unless indicated otherwise. The following commercial antibodies were used: Huntingtin (WB-1:3000 clone 1HU-4C8, no. MAB2166), was obtained from Millipore-Sigma. Antibodies for DARPP-32 (WB-1:20000, no. 2306) mTOR (WB-1:3000, no. 2983), pS6K (WB-1:1000, no. 9234), S6K (WB-1;1000, no. 9202), p4EBP1 (WB-1:1000, no 9451), 4EBP1 (WB-1:15000, no. 9644), Rheb (1:2000, no. 13187), p62 (WB-1:1000, no. 39749), and LC3B (WB-1:2000, IHC-1:200, no. 3868) were from Cell Signaling Technology. Antibody against GFAP (WB-1:2000, no. 13-0300) was from ThermoFisher Scientific. Rhes antibody (WB-1:1000, RHES-101AP) was from Fabgennix. Antibodies for β-actin (WB-1:20,000; no. sc-47778), was obtained from Santa Cruz Biotechnology. HRP-conjugated secondary antibodies: goat anti-mouse (1:10,000; no.115-035-146), and goat anti-rabbit (1:10,000; no. 111-035-144) were from Jackson ImmunoResearch Inc.

Animals

Hdh150Q knock in knock-in heterozygous (B6.129P2-*Htt*^{tm2Detl}/150J # 004595) and C57BL/6J (JR # 000664) control mice were from The Jackson laboratory, Bar Harbor, ME. Rhes KO mice were from Alessandro Usiello were bred to produce Hdh150Q-Rhes KO and littermate groups, Hdh150Q (HD Het and HD homo), Rhes KO and WT, and the genotypes were confirmed by an established PCR protocol, as described before[45]. Behavior evaluation was performed as indicated before[55]. Number of animals used are indicated in Table 1.

Table 1. Number of animals used

Genotype	*80 weeks*	*100 weeks*
Rhes WT/HD-het	19	12
	(11 male)	(7 male)
Rhes KO/HD-het	14	12
	(7 male)	(7 male)
Rhes KO/HD-homo	10	7
	(5 male)	(2 male)
Rhes KO/WT	12	9
	(5 male)	(3 male)
Rhes WT/HD-homo	10	6
	(3 male)	(1 male)
WT	9	5
	(4 male)	(2 male)

Behavioral assay

Behavioral testing was performed by the experimenter in an unbiased and blinded manner for the animal's genotype. All behavioral testing was performed during the light phase of the light-dark cycle (8:00 a.m. and 12:00 p.m), as described before[55]. Rotarod output was measured on day 1, open field on day 2, and the battery of behavioral tests on day 3 of each week of behavioral testing, to avoid variability in time of testing.

Rotarod

Every month, rotarod behavioral assay was conducted using a linear accelerating rotation paradigm (Med Associates Inc.) in three trials separated by 20 minutes. The mice were placed on the apparatus at 4 rpm and were subjected to increasing rpm, accelerating to 40 rpm over the course of a maximum of 5 min. The average of the three trials over four days was used to measure each mouse's total latency to fall.

Open field activity

EthoVision XT software (Noldus Information Technology) was used to measure total distance traveled and velocity of mice during a single 30-minute session in which a mouse was positioned in the center of a square enclosure and total distance traveled was measured.

Behavioral battery

Subjective behavioral testing was adapted from a previous report[55, 77]. The battery of tests, each performed in triplicate, measured ledge walking, clasping, gait, kyphosis, and

tremor. Individual measures were graded on a scale of 0 (no phenotype) to 3 (worst manifestation), as previously mentioned[55, 77]. To determine tremor, mice were placed in a clean cage and observed for 30 s. Each mouse was scored as follows: 0, no signs of tremor; 1, present but mild tremor; 2, severe intervals of tremor or constant moderate tremor; 3, outrageous chronic tremor. The mean of all five behavioral battery tests was used to create the composite ranking. Behaviors procedures were approved by the Scripps Research Institute Florida Institutional Animal Care and Use Committee.

Western blotting

Western blotting from striatal tissue were carried as described before[78, 79]. Striatal tissue was rinsed briefly in PBS and directly lysed in lysis buffer [50 mM Tris-HCl (pH 7.4), 150 mM NaCl, 1% Triton X-100, 1x protease inhibitor cocktail (Roche, Sigma) and 1x phosphatase inhibitor (PhosStop, Roche, Sigma)], sonicated for 2 x 5 sec at 20% amplitude, and cleared by centrifugation for 10 min at 11,000 g at 4°C. Striatal cells or human fibroblasts were lysed in radioimmunoprecipitation assay (RIPA)buffer [50 mM Tris-HCl (pH 7.4), 150 mM NaCl, 1.0% Triton X-100, 0.5% sodium deoxycholate, 0.1% SDS] with 1x complete protease inhibitor cocktail and 1x phosphatase inhibitor , followed by a brief sonication for 2 x 5 sec at 30% amplitude and cleared by centrifugation for 10 min at 11,000g at 4°C. Protein concentration was determined with a bicinchoninic acid (BCA) protein assay reagent (Pierce). Equal amounts of protein (20-50 µg) were loaded and were separated by electrophoresis in 4 to 12% Bis-Tris Gel (ThermoFisher Scientific), transferred to polyvinylidene difluoride membranes, and probed with the indicated primary antibodies. HRP-conjugated secondary antibodies were probed to detect bound primary IgG with a chemiluminescence imager (Alpha Innotech) using enhanced chemiluminescence from WesternBright Quantum (Advansta) The band intensities were quantified with ImageJ software (NIH). Total proteins were then normalized to actin. Phosphorylated proteins to their respective total proteins.

Statistical analysis

Data are presented as mean ± SEM as indicated. Except where stated all experiments were performed at least in biological triplicate and repeated at least twice. The mouse

behavioral and the data analysis was carried out in a blinded manner. Images were quantified using ImageJ (FIJI). Behavioral data consisted of categorical and continuous outcomes. Categorical data was analyzed using Fisher's Exact test. Statistical comparison was performed between groups using two-tailed Student's t-test, one-way analysis of variance (ANOVA) followed by Tukey's multiple comparison test. Significance was set at $p < 0.05$. All statistical tests were performed using Prism 9.0 (GraphPad software).

Acknowledgments: We would like to thank Melissa Benilous for her administrative help and the members of the lab for their continuous support and collaborative atmosphere. We like to thank members at the Scripps proteomics and genomic core for their help and expertise. This research was supported by grant awards from NIH/NINDS R01-NS087019-01A1, NIH/NINDS R01-NS094577-01A1, a grant from Cure for Huntington Disease Research Initiative (CHDI) foundation and Scripps bridge funding.

Author contributions: S.S conceptualized the project and co-designed experiments with J. H and N. S who performed mouse behavior. N.S performed western blotting experiments and analyzed the data. Sw. S. carried out breeding and assisted in the behavioral analysis. S.S wrote the manuscript with inputs from coauthors.

Figure Legends:

Figure 1. Effect of Rhes deletion on age-associated motor abnormalities in Hdh150Q KI HD mice. (A) Body weight, (B), rotarod, (C) open field (D) behavioral battery composite score included ledge-test, clasping, gait, kyphosis, and tremor evaluation. The frequency of each behavior according to the genotype is shown in F, a composite score for all the behavioral battery is shown in G. Data are mean ± SEM (n = 5-19/genotype). *P<0.05, **P<0.01, ****P< 0.0001, 2way ANOVA followed by Tukey's multiple comparison test.

Figure 2: Biochemical alterations of Rhes deletion in 103 weeks old Hdh150Q KI heterozygous mice. (A) Western blot analysis of indicated proteins from striatum of indicated mice in $Hdh^{150Q/+}$ heterozygous and other mice groups. (B-E) Bar graph shows

quantification of the indicated proteins from E. Data are mean ± SEM, n = 3-4 per group, *P<0.05, **P<0.01, one-way ANOVA followed by Tukey's multiple comparison test.

Figure 3: Biochemical alterations of Rhes deletion in 103 weeks old Hdh150Q KI homozygous mice. (A) Western blot analysis of indicated proteins from striatum of indicated mice in $Hdh^{150Q/150Q}$ homozygous and other mice group. (B-E) Bar graph shows quantification of the indicated proteins from E. Data are mean ± SEM, n = 3-4 per group, *P<0.05, **P<0.01, ***P< 0.001, ****P< 0.0001, one-way ANOVA followed by Tukey's multiple comparison test.

References

1. Vonsattel JP, DiFiglia M. Huntington disease. J Neuropathol Exp Neurol. 1998;57(5):369-84. Epub 1998/05/22. doi: 10.1097/00005072-199805000-00001. PubMed PMID: 9596408.
2. Ross CA, Tabrizi SJ. Huntington's disease: from molecular pathogenesis to clinical treatment. Lancet Neurol. 2011;10(1):83-98. Epub 2010/12/18. doi: 10.1016/S1474-4422(10)70245-3. PubMed PMID: 21163446.
3. Rosas HD, Salat DH, Lee SY, Zaleta AK, Pappu V, Fischl B, Greve D, Hevelone N, Hersch SM. Cerebral cortex and the clinical expression of Huntington's disease: complexity and heterogeneity. Brain. 2008;131(Pt 4):1057-68. Epub 2008/03/14. doi: 10.1093/brain/awn025. PubMed PMID: 18337273; PMCID: PMC2657201.
4. Mielcarek M. Huntington's disease is a multi-system disorder. Rare Dis. 2015;3(1):e1058464. Epub 2015/10/16. doi: 10.1080/21675511.2015.1058464. PubMed PMID: 26459693; PMCID: PMC4588536.
5. DiFiglia M, Sapp E, Chase K, Schwarz C, Meloni A, Young C, Martin E, Vonsattel JP, Carraway R, Reeves SA, et al. Huntingtin is a cytoplasmic protein associated with vesicles in human and rat brain neurons. Neuron. 1995;14(5):1075-81. Epub 1995/05/01. doi: 10.1016/0896-6273(95)90346-1. PubMed PMID: 7748555.
6. Hoffner G, Kahlem P, Djian P. Perinuclear localization of huntingtin as a consequence of its binding to microtubules through an interaction with beta-tubulin: relevance to Huntington's disease. J Cell Sci. 2002;115(Pt 5):941-8. Epub 2002/03/01. PubMed PMID: 11870213.
7. Velier J, Kim M, Schwarz C, Kim TW, Sapp E, Chase K, Aronin N, DiFiglia M. Wild-type and mutant huntingtins function in vesicle trafficking in the secretory and endocytic pathways. Exp Neurol. 1998;152(1):34-40. Epub 1998/07/31. doi: 10.1006/exnr.1998.6832. PubMed PMID: 9682010.
8. Brandstaetter H, Kruppa AJ, Buss F. Huntingtin is required for ER-to-Golgi transport and for secretory vesicle fusion at the plasma membrane. Dis Model Mech. 2014;7(12):1335-40. Epub 2014/11/05. doi: 10.1242/dmm.017368. PubMed PMID: 25368120; PMCID: PMC4257002.

9. Xia J, Lee DH, Taylor J, Vandelft M, Truant R. Huntingtin contains a highly conserved nuclear export signal. Hum Mol Genet. 2003;12(12):1393-403. Epub 2003/06/05. doi: 10.1093/hmg/ddg156. PubMed PMID: 12783847.
10. Kegel KB, Meloni AR, Yi Y, Kim YJ, Doyle E, Cuiffo BG, Sapp E, Wang Y, Qin ZH, Chen JD, Nevins JR, Aronin N, DiFiglia M. Huntingtin is present in the nucleus, interacts with the transcriptional corepressor C-terminal binding protein, and represses transcription. J Biol Chem. 2002;277(9):7466-76. Epub 2001/12/12. doi: 10.1074/jbc.M103946200. PubMed PMID: 11739372.
11. Zuccato C, Ciammola A, Rigamonti D, Leavitt BR, Goffredo D, Conti L, MacDonald ME, Friedlander RM, Silani V, Hayden MR, Timmusk T, Sipione S, Cattaneo E. Loss of huntingtin-mediated BDNF gene transcription in Huntington's disease. Science. 2001;293(5529):493-8. Epub 2001/06/16. doi: 10.1126/science.1059581. PubMed PMID: 11408619.
12. Sipione S, Rigamonti D, Valenza M, Zuccato C, Conti L, Pritchard J, Kooperberg C, Olson JM, Cattaneo E. Early transcriptional profiles in huntingtin-inducible striatal cells by microarray analyses. Hum Mol Genet. 2002;11(17):1953-65. Epub 2002/08/08. doi: 10.1093/hmg/11.17.1953. PubMed PMID: 12165557.
13. Nucifora FC, Jr., Sasaki M, Peters MF, Huang H, Cooper JK, Yamada M, Takahashi H, Tsuji S, Troncoso J, Dawson VL, Dawson TM, Ross CA. Interference by huntingtin and atrophin-1 with cbp-mediated transcription leading to cellular toxicity. Science. 2001;291(5512):2423-8. Epub 2001/03/27. doi: 10.1126/science.1056784. PubMed PMID: 11264541.
14. Zhang H, Das S, Li QZ, Dragatsis I, Repa J, Zeitlin S, Hajnoczky G, Bezprozvanny I. Elucidating a normal function of huntingtin by functional and microarray analysis of huntingtin-null mouse embryonic fibroblasts. BMC Neurosci. 2008;9:38. Epub 2008/04/17. doi: 10.1186/1471-2202-9-38. PubMed PMID: 18412970; PMCID: PMC2377268.
15. Takano H, Gusella JF. The predominantly HEAT-like motif structure of huntingtin and its association and coincident nuclear entry with dorsal, an NF-kB/Rel/dorsal family transcription factor. BMC Neurosci. 2002;3:15. Epub 2002/10/16. doi: 10.1186/1471-2202-3-15. PubMed PMID: 12379151; PMCID: PMC137586.
16. Steffan JS, Kazantsev A, Spasic-Boskovic O, Greenwald M, Zhu YZ, Gohler H, Wanker EE, Bates GP, Housman DE, Thompson LM. The Huntington's disease protein interacts with p53 and CREB-binding protein and represses transcription. Proc Natl Acad Sci U S A. 2000;97(12):6763-8. Epub 2000/05/24. doi: 10.1073/pnas.100110097. PubMed PMID: 10823891; PMCID: PMC18731.
17. Paul BD, Sbodio JI, Xu R, Vandiver MS, Cha JY, Snowman AM, Snyder SH. Cystathionine gamma-lyase deficiency mediates neurodegeneration in Huntington's disease. Nature. 2014;509(7498):96-100. Epub 2014/03/29. doi: 10.1038/nature13136. PubMed PMID: 24670645; PMCID: PMC4349202.
18. Sbodio JI, Snyder SH, Paul BD. Transcriptional control of amino acid homeostasis is disrupted in Huntington's disease. Proc Natl Acad Sci U S A. 2016;113(31):8843-8. Epub 2016/07/21. doi: 10.1073/pnas.1608264113. PubMed PMID: 27436896; PMCID: PMC4978294.
19. Graham RK, Deng Y, Slow EJ, Haigh B, Bissada N, Lu G, Pearson J, Shehadeh J, Bertram L, Murphy Z, Warby SC, Doty CN, Roy S, Wellington CL, Leavitt BR, Raymond LA, Nicholson DW, Hayden MR. Cleavage at the caspase-6 site is required for neuronal dysfunction

and degeneration due to mutant huntingtin. Cell. 2006;125(6):1179-91. Epub 2006/06/17. doi: 10.1016/j.cell.2006.04.026. PubMed PMID: 16777606.
20. O'Brien R, DeGiacomo F, Holcomb J, Bonner A, Ring KL, Zhang N, Zafar K, Weiss A, Lager B, Schilling B, Gibson BW, Chen S, Kwak S, Ellerby LM. Integration-independent Transgenic Huntington Disease Fragment Mouse Models Reveal Distinct Phenotypes and Life Span in Vivo. J Biol Chem. 2015;290(31):19287-306. Epub 2015/05/31. doi: 10.1074/jbc.M114.623561. PubMed PMID: 26025364; PMCID: PMC4521048.
21. Panov AV, Gutekunst CA, Leavitt BR, Hayden MR, Burke JR, Strittmatter WJ, Greenamyre JT. Early mitochondrial calcium defects in Huntington's disease are a direct effect of polyglutamines. Nat Neurosci. 2002;5(8):731-6. Epub 2002/06/29. doi: 10.1038/nn884. PubMed PMID: 12089530.
22. Pchitskaya E, Popugaeva E, Bezprozvanny I. Calcium signaling and molecular mechanisms underlying neurodegenerative diseases. Cell Calcium. 2018;70:87-94. Epub 2017/07/22. doi: 10.1016/j.ceca.2017.06.008. PubMed PMID: 28728834; PMCID: PMC5748019.
23. Sciamanna G, Napolitano F, Pelosi B, Bonsi P, Vitucci D, Nuzzo T, Punzo D, Ghiglieri V, Ponterio G, Pasqualetti M, Pisani A, Usiello A. Rhes regulates dopamine D2 receptor transmission in striatal cholinergic interneurons. Neurobiol Dis. 2015;78:146-61. Epub 2015/03/31. doi: 10.1016/j.nbd.2015.03.021. PubMed PMID: 25818655.
24. Ghiglieri V, Napolitano F, Pelosi B, Schepisi C, Migliarini S, Di Maio A, Pendolino V, Mancini M, Sciamanna G, Vitucci D, Maddaloni G, Giampa C, Errico F, Nistico R, Pasqualetti M, Picconi B, Usiello A. Rhes influences striatal cAMP/PKA-dependent signaling and synaptic plasticity in a gender-sensitive fashion. Sci Rep. 2015;5:10933. Epub 2015/07/21. doi: 10.1038/srep10933. PubMed PMID: 26190541; PMCID: PMC4507147.
25. Harrison LM. Rhes: a GTP-binding protein integral to striatal physiology and pathology. Cell Mol Neurobiol. 2012;32(6):907-18. Epub 2012/03/28. doi: 10.1007/s10571-012-9830-6. PubMed PMID: 22450871; PMCID: PMC3396771.
26. Usui H, Falk JD, Dopazo A, de Lecea L, Erlander MG, Sutcliffe JG. Isolation of clones of rat striatum-specific mRNAs by directional tag PCR subtraction. J Neurosci. 1994;14(8):4915-26. Epub 1994/08/01. PubMed PMID: 8046460; PMCID: PMC6577190.
27. Vargiu P, De Abajo R, Garcia-Ranea JA, Valencia A, Santisteban P, Crespo P, Bernal J. The small GTP-binding protein, Rhes, regulates signal transduction from G protein-coupled receptors. Oncogene. 2004;23(2):559-68. Epub 2004/01/16. doi: 10.1038/sj.onc.1207161. PubMed PMID: 14724584.
28. Errico F, Santini E, Migliarini S, Borgkvist A, Centonze D, Nasti V, Carta M, De Chiara V, Prosperetti C, Spano D, Herve D, Pasqualetti M, Di Lauro R, Fisone G, Usiello A. The GTP-binding protein Rhes modulates dopamine signalling in striatal medium spiny neurons. Mol Cell Neurosci. 2008;37(2):335-45. Epub 2007/11/24. doi: 10.1016/j.mcn.2007.10.007. PubMed PMID: 18035555.
29. Harrison LM, He Y. Rhes and AGS1/Dexras1 affect signaling by dopamine D1 receptors through adenylyl cyclase. J Neurosci Res. 2011;89(6):874-82. Epub 2011/03/05. doi: 10.1002/jnr.22604. PubMed PMID: 21374700; PMCID: PMC3077464.
30. Subramaniam S, Napolitano F, Mealer RG, Kim S, Errico F, Barrow R, Shahani N, Tyagi R, Snyder SH, Usiello A. Rhes, a striatal-enriched small G protein, mediates mTOR signaling and L-DOPA-induced dyskinesia. Nat Neurosci. 2011;15(2):191-3. Epub 2011/12/20. doi: 10.1038/nn.2994. PubMed PMID: 22179112; PMCID: PMC3267880.

31. Brugnoli A, Napolitano F, Usiello A, Morari M. Genetic deletion of Rhes or pharmacological blockade of mTORC1 prevent striato-nigral neurons activation in levodopa-induced dyskinesia. Neurobiol Dis. 2016;85:155-63. Epub 2015/11/03. doi: 10.1016/j.nbd.2015.10.020. PubMed PMID: 26522958.
32. Subramaniam S, Mealer RG, Sixt KM, Barrow RK, Usiello A, Snyder SH. Rhes, a physiologic regulator of sumoylation, enhances cross-sumoylation between the basic sumoylation enzymes E1 and Ubc9. J Biol Chem. 2010;285(27):20428-32. Epub 2010/04/29. doi: 10.1074/jbc.C110.127191. PubMed PMID: 20424159; PMCID: PMC2898300.
33. Rivera O SM, Shahani N, Ramírez-Jarquín UN, Crynen G, Karunadharma P, McManus F, Pierre T, Subramaniam S. Rhes, a Striatal Enriched Protein, Regulates Post-Translational Small-Ubiquitin-like-Modifier (SUMO) Modification of Nuclear Proteins and Alters Gene Expression2020. doi: https://doi.org/10.1101/2020.06.18.160044.
34. Subramaniam S, Sixt KM, Barrow R, Snyder SH. Rhes, a striatal specific protein, mediates mutant-huntingtin cytotoxicity. Science. 2009;324(5932):1327-30. Epub 2009/06/06. doi: 10.1126/science.1172871. PubMed PMID: 19498170; PMCID: PMC2745286.
35. O'Rourke JG, Gareau JR, Ochaba J, Song W, Rasko T, Reverter D, Lee J, Monteys AM, Pallos J, Mee L, Vashishtha M, Apostol BL, Nicholson TP, Illes K, Zhu YZ, Dasso M, Bates GP, Difiglia M, Davidson B, Wanker EE, Marsh JL, Lima CD, Steffan JS, Thompson LM. SUMO-2 and PIAS1 modulate insoluble mutant huntingtin protein accumulation. Cell Rep. 2013;4(2):362-75. Epub 2013/07/23. doi: 10.1016/j.celrep.2013.06.034. PubMed PMID: 23871671; PMCID: PMC3931302.
36. Okamoto S, Pouladi MA, Talantova M, Yao D, Xia P, Ehrnhoefer DE, Zaidi R, Clemente A, Kaul M, Graham RK, Zhang D, Vincent Chen HS, Tong G, Hayden MR, Lipton SA. Balance between synaptic versus extrasynaptic NMDA receptor activity influences inclusions and neurotoxicity of mutant huntingtin. Nat Med. 2009;15(12):1407-13. Epub 2009/11/17. doi: 10.1038/nm.2056. PubMed PMID: 19915593; PMCID: PMC2789858.
37. Seredenina T, Gokce O, Luthi-Carter R. Decreased striatal RGS2 expression is neuroprotective in Huntington's disease (HD) and exemplifies a compensatory aspect of HD-induced gene regulation. PLoS One. 2011;6(7):e22231. Epub 2011/07/23. doi: 10.1371/journal.pone.0022231. PubMed PMID: 21779398; PMCID: PMC3136499.
38. Sbodio JI, Paul BD, Machamer CE, Snyder SH. Golgi protein ACBD3 mediates neurotoxicity associated with Huntington's disease. Cell Rep. 2013;4(5):890-7. Epub 2013/09/10. doi: 10.1016/j.celrep.2013.08.001. PubMed PMID: 24012756; PMCID: PMC3801179.
39. Lu B, Palacino J. A novel human embryonic stem cell-derived Huntington's disease neuronal model exhibits mutant huntingtin (mHTT) aggregates and soluble mHTT-dependent neurodegeneration. FASEB J. 2013;27(5):1820-9. Epub 2013/01/18. doi: 10.1096/fj.12-219220. PubMed PMID: 23325320.
40. Argenti M. THE ROLE OF MITOCHONDRIAL DYSFUNCTION IN HUNTINGTON'S DISEASE PATHOGENESIS AND ITS RELATION WITH STRIATAL RHES PROTEIN. PhD Thesis, Università degli Studi di Padova, Padova PD, Italy. 2014.
41. Hernandez I, Luna G, Rauch JN, Reis SA, Giroux M, Karch CM, Boctor D, Sibih YE, Storm NJ, Diaz A, Kaushik S, Zekanowski C, Kang AA, Hinman CR, Cerovac V, Guzman E, Zhou H, Haggarty SJ, Goate AM, Fisher SK, Cuervo AM, Kosik KS. A farnesyltransferase inhibitor activates lysosomes and reduces tau pathology in mice with tauopathy. Sci Transl Med. 2019;11(485). Epub 2019/03/29. doi: 10.1126/scitranslmed.aat3005. PubMed PMID: 30918111.

42. Alexander J. Ehrenberg KL, Israel Hernandez, Caroline Lew, William W. Seeley, Salvatore Spina, Bruce Miller, Helmut Heinsen, Martin Kampmann, Kenneth S. Kosik, Lea T. Grinberg. Mislocalization and clearance of neuronal Rhes as a novel hallmark of tauopathies. medRxiv. 2020. doi: https://doi.org/10.1101/2020.10.27.20220954
43. Sharma M, Subramaniam S. Rhes travels from cell to cell and transports Huntington disease protein via TNT-like protrusion. J Cell Biol. 2019;218(6):1972-93. Epub 2019/05/12. doi: 10.1083/jcb.201807068. PubMed PMID: 31076452; PMCID: PMC6548131.
44. Sharma M, Jarquin UNR, Rivera O, Kazantzis M, Eshraghi M, Shahani N, Sharma V, Tapia R, Subramaniam S. Rhes, a striatal-enriched protein, promotes mitophagy via Nix. Proc Natl Acad Sci U S A. 2019;116(47):23760-71. Epub 2019/11/05. doi: 10.1073/pnas.1912868116. PubMed PMID: 31676548; PMCID: PMC6876193.
45. Swarnkar S, Chen Y, Pryor WM, Shahani N, Page DT, Subramaniam S. Ectopic expression of the striatal-enriched GTPase Rhes elicits cerebellar degeneration and an ataxia phenotype in Huntington's disease. Neurobiol Dis. 2015;82:66-77. Epub 2015/06/07. doi: 10.1016/j.nbd.2015.05.011. PubMed PMID: 26048156.
46. Baiamonte BA, Lee FA, Brewer ST, Spano D, LaHoste GJ. Attenuation of Rhes activity significantly delays the appearance of behavioral symptoms in a mouse model of Huntington's disease. PLoS One. 2013;8(1):e53606. Epub 2013/01/26. doi: 10.1371/journal.pone.0053606. PubMed PMID: 23349722; PMCID: PMC3549908.
47. Heng MY, Tallaksen-Greene SJ, Detloff PJ, Albin RL. Longitudinal evaluation of the Hdh(CAG)150 knock-in murine model of Huntington's disease. J Neurosci. 2007;27(34):8989-98. Epub 2007/08/24. doi: 10.1523/JNEUROSCI.1830-07.2007. PubMed PMID: 17715336; PMCID: PMC6672210.
48. Southwell AL, Smith-Dijak A, Kay C, Sepers M, Villanueva EB, Parsons MP, Xie Y, Anderson L, Felczak B, Waltl S, Ko S, Cheung D, Dal Cengio L, Slama R, Petoukhov E, Raymond LA, Hayden MR. An enhanced Q175 knock-in mouse model of Huntington disease with higher mutant huntingtin levels and accelerated disease phenotypes. Hum Mol Genet. 2016;25(17):3654-75. Epub 2016/07/06. doi: 10.1093/hmg/ddw212. PubMed PMID: 27378694; PMCID: PMC5216613.
49. Liu Q, Cheng S, Yang H, Zhu L, Pan Y, Jing L, Tang B, Li S, Li XJ. Loss of Hap1 selectively promotes striatal degeneration in Huntington disease mice. Proc Natl Acad Sci U S A. 2020;117(33):20265-73. Epub 2020/08/05. doi: 10.1073/pnas.2002283117. PubMed PMID: 32747555; PMCID: PMC7443904.
50. Steffan JS, Agrawal N, Pallos J, Rockabrand E, Trotman LC, Slepko N, Illes K, Lukacsovich T, Zhu YZ, Cattaneo E, Pandolfi PP, Thompson LM, Marsh JL. SUMO modification of Huntingtin and Huntington's disease pathology. Science. 2004;304(5667):100-4. Epub 2004/04/06. doi: 10.1126/science.1092194. PubMed PMID: 15064418.
51. Lee JH, Sowada MJ, Boudreau RL, Aerts AM, Thedens DR, Nopoulos P, Davidson BL. Rhes suppression enhances disease phenotypes in Huntington's disease mice. J Huntingtons Dis. 2014;3(1):65-71. Epub 2014/07/27. doi: 10.3233/JHD-140094. PubMed PMID: 25062765; PMCID: PMC4139702.
52. Lee JH, Tecedor L, Chen YH, Monteys AM, Sowada MJ, Thompson LM, Davidson BL. Reinstating aberrant mTORC1 activity in Huntington's disease mice improves disease phenotypes. Neuron. 2015;85(2):303-15. Epub 2015/01/06. doi: 10.1016/j.neuron.2014.12.019. PubMed PMID: 25556834; PMCID: PMC4355620.

53. Erie C, Sacino M, Houle L, Lu ML, Wei J. Altered lysosomal positioning affects lysosomal functions in a cellular model of Huntington's disease. Eur J Neurosci. 2015;42(3):1941-51. Epub 2015/05/23. doi: 10.1111/ejn.12957. PubMed PMID: 25997742; PMCID: PMC4523460.
54. Abd-Elrahman KS, Ferguson SSG. Modulation of mTOR and CREB pathways following mGluR5 blockade contribute to improved Huntington's pathology in zQ175 mice. Mol Brain. 2019;12(1):35. Epub 2019/04/10. doi: 10.1186/s13041-019-0456-1. PubMed PMID: 30961637; PMCID: PMC6454676.
55. Pryor WM, Biagioli M, Shahani N, Swarnkar S, Huang WC, Page DT, MacDonald ME, Subramaniam S. Huntingtin promotes mTORC1 signaling in the pathogenesis of Huntington's disease. Sci Signal. 2014;7(349):ra103. Epub 2014/10/30. doi: 10.1126/scisignal.2005633. PubMed PMID: 25351248.
56. Wang T, Lao U, Edgar BA. TOR-mediated autophagy regulates cell death in Drosophila neurodegenerative disease. J Cell Biol. 2009;186(5):703-11. Epub 2009/09/02. doi: 10.1083/jcb.200904090. PubMed PMID: 19720874; PMCID: PMC2742187.
57. Steventon JJ, Trueman RC, Ma D, Yhnell E, Bayram-Weston Z, Modat M, Cardoso J, Ourselin S, Lythgoe M, Stewart A, Rosser AE, Jones DK. Longitudinal in vivo MRI in a Huntington's disease mouse model: Global atrophy in the absence of white matter microstructural damage. Sci Rep. 2016;6:32423. Epub 2016/09/02. doi: 10.1038/srep32423. PubMed PMID: 27581950; PMCID: PMC5007531.
58. Brooks S, Higgs G, Jones L, Dunnett SB. Longitudinal analysis of the behavioural phenotype in Hdh(CAG)150 Huntington's disease knock-in mice. Brain Res Bull. 2012;88(2-3):182-8. Epub 2010/05/12. doi: 10.1016/j.brainresbull.2010.05.004. PubMed PMID: 20457230.
59. Croce KR, Yamamoto A. A role for autophagy in Huntington's disease. Neurobiol Dis. 2019;122:16-22. Epub 2018/08/28. doi: 10.1016/j.nbd.2018.08.010. PubMed PMID: 30149183; PMCID: PMC6364695.
60. Valadao PAC, Santos KBS, Ferreira EVTH, Macedo ECT, Teixeira AL, Guatimosim C, de Miranda AS. Inflammation in Huntington's disease: A few new twists on an old tale. J Neuroimmunol. 2020;348:577380. Epub 2020/09/09. doi: 10.1016/j.jneuroim.2020.577380. PubMed PMID: 32896821.
61. Aspuria PJ, Tamanoi F. The Rheb family of GTP-binding proteins. Cell Signal. 2004;16(10):1105-12. Epub 2004/07/09. doi: 10.1016/j.cellsig.2004.03.019. PubMed PMID: 15240005.
62. Qin X, Jiang B, Zhang Y. 4E-BP1, a multifactor regulated multifunctional protein. Cell Cycle. 2016;15(6):781-6. Epub 2016/02/24. doi: 10.1080/15384101.2016.1151581. PubMed PMID: 26901143; PMCID: PMC4845917.
63. Schilling G, Becher MW, Sharp AH, Jinnah HA, Duan K, Kotzuk JA, Slunt HH, Ratovitski T, Cooper JK, Jenkins NA, Copeland NG, Price DL, Ross CA, Borchelt DR. Intranuclear inclusions and neuritic aggregates in transgenic mice expressing a mutant N-terminal fragment of huntingtin. Hum Mol Genet. 1999;8(3):397-407. Epub 1999/02/09. doi: 10.1093/hmg/8.3.397. PubMed PMID: 9949199.
64. Jiang W, Wei W, Gaertig MA, Li S, Li XJ. Therapeutic Effect of Berberine on Huntington's Disease Transgenic Mouse Model. PLoS One. 2015;10(7):e0134142. Epub 2015/08/01. doi: 10.1371/journal.pone.0134142. PubMed PMID: 26225560; PMCID: PMC4520448.

65. Zhang J, Peng Q, Li Q, Jahanshad N, Hou Z, Jiang M, Masuda N, Langbehn DR, Miller MI, Mori S, Ross CA, Duan W. Longitudinal characterization of brain atrophy of a Huntington's disease mouse model by automated morphological analyses of magnetic resonance images. Neuroimage. 2010;49(3):2340-51. Epub 2009/10/24. doi: 10.1016/j.neuroimage.2009.10.027. PubMed PMID: 19850133; PMCID: PMC2929697.
66. Mangiarini L, Sathasivam K, Seller M, Cozens B, Harper A, Hetherington C, Lawton M, Trottier Y, Lehrach H, Davies SW, Bates GP. Exon 1 of the HD gene with an expanded CAG repeat is sufficient to cause a progressive neurological phenotype in transgenic mice. Cell. 1996;87(3):493-506. Epub 1996/11/01. doi: 10.1016/s0092-8674(00)81369-0. PubMed PMID: 8898202.
67. Bayram-Weston Z, Jones L, Dunnett SB, Brooks SP. Light and electron microscopic characterization of the evolution of cellular pathology in HdhQ92 Huntington's disease knock-in mice. Brain Res Bull. 2012;88(2-3):171-81. Epub 2011/04/26. doi: 10.1016/j.brainresbull.2011.03.013. PubMed PMID: 21513775.
68. Crook ZR, Housman D. Huntington's disease: can mice lead the way to treatment? Neuron. 2011;69(3):423-35. Epub 2011/02/15. doi: 10.1016/j.neuron.2010.12.035. PubMed PMID: 21315254; PMCID: PMC4685469.
69. Subramaniam S, Snyder SH. Huntington's disease is a disorder of the corpus striatum: focus on Rhes (Ras homologue enriched in the striatum). Neuropharmacology. 2011;60(7-8):1187-92. Epub 2010/11/04. doi: 10.1016/j.neuropharm.2010.10.025. PubMed PMID: 21044641.
70. Subramaniam S. Selective Neuronal Death in Neurodegenerative Diseases: The Ongoing Mystery. Yale J Biol Med. 2019;92(4):695-705. Epub 2019/12/24. PubMed PMID: 31866784; PMCID: PMC6913821.
71. Feyder M, Plewnia C, Lieberman OJ, Spigolon G, Piccin A, Urbina L, Dehay B, Li Q, Nilsson P, Altun M, Santini E, Sulzer D, Bezard E, Borgkvist A, Fisone G. Involvement of Autophagy in Levodopa-Induced Dyskinesia. Mov Disord. 2021. Epub 2021/01/19. doi: 10.1002/mds.28480. PubMed PMID: 33460487.
72. Mealer RG, Murray AJ, Shahani N, Subramaniam S, Snyder SH. Rhes, a striatal-selective protein implicated in Huntington disease, binds beclin-1 and activates autophagy. J Biol Chem. 2014;289(6):3547-54. Epub 2013/12/11. doi: 10.1074/jbc.M113.536912. PubMed PMID: 24324270; PMCID: PMC3916556.
73. Park S RJU, Shahani N, Rivera O, Sharma M, McManus FP, Thibault P, Subramaniam S. SUMO Modifies GβL and Mediates mTOR Signaling. BioRxiv. 2020. doi: https://doi.org/10.1101/2020.09.03.281881.
74. Uri Nimrod Ramírez-Jarquín MS, Neelam Shahani, Srinivasa Subramaniam. Deletion of Small Ubiquitin-like Modifier-1 Attenuates Behavioral and Anatomical Deficits by Enhancing Functional Autophagic Activities in Huntington Disease. BioRxiv. 2021. doi: https://doi.org/10.1101/2021.02.15.431277
75. Ravikumar B, Vacher C, Berger Z, Davies JE, Luo S, Oroz LG, Scaravilli F, Easton DF, Duden R, O'Kane CJ, Rubinsztein DC. Inhibition of mTOR induces autophagy and reduces toxicity of polyglutamine expansions in fly and mouse models of Huntington disease. Nat Genet. 2004;36(6):585-95. Epub 2004/05/18. doi: 10.1038/ng1362. PubMed PMID: 15146184.
76. Traisupa A, Wongba C, Taylor DN. AIDS and prevalence of antibody to human immunodeficiency virus (HIV) in high risk groups in Thailand. Genitourin Med.

1987;63(2):106-8. Epub 1987/04/01. doi: 10.1136/sti.63.2.106. PubMed PMID: 3646990; PMCID: PMC1194028.

77. Guyenet SJ, Furrer SA, Damian VM, Baughan TD, La Spada AR, Garden GA. A simple composite phenotype scoring system for evaluating mouse models of cerebellar ataxia. J Vis Exp. 2010(39). Epub 2010/05/25. doi: 10.3791/1787. PubMed PMID: 20495529; PMCID: PMC3121238.

78. Eshraghi M, Ramirez-Jarquin UN, Shahani N, Nuzzo T, De Rosa A, Swarnkar S, Galli N, Rivera O, Tsaprailis G, Scharager-Tapia C, Crynen G, Li Q, Thiolat ML, Bezard E, Usiello A, Subramaniam S. RasGRP1 is a causal factor in the development of l-DOPA-induced dyskinesia in Parkinson's disease. Sci Adv. 2020;6(18):eaaz7001. Epub 2020/05/20. doi: 10.1126/sciadv.aaz7001. PubMed PMID: 32426479; PMCID: PMC7195186.

79. Ramirez-Jarquin UN, Shahani N, Pryor W, Usiello A, Subramaniam S. The mammalian target of rapamycin (mTOR) kinase mediates haloperidol-induced cataleptic behavior. Transl Psychiatry. 2020;10(1):336. Epub 2020/10/04. doi: 10.1038/s41398-020-01014-x. PubMed PMID: 33009372.

Figure 1

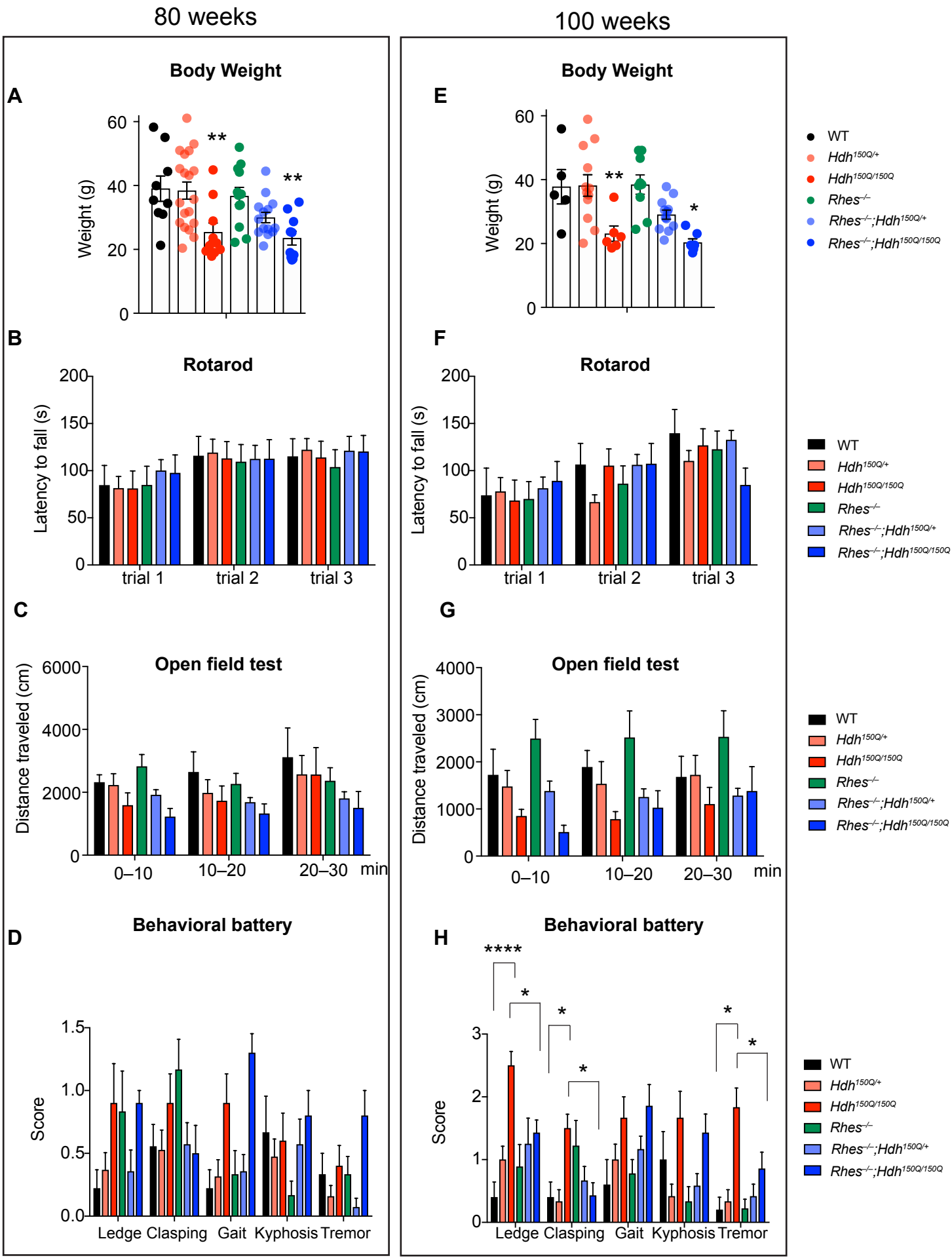

Figure 2

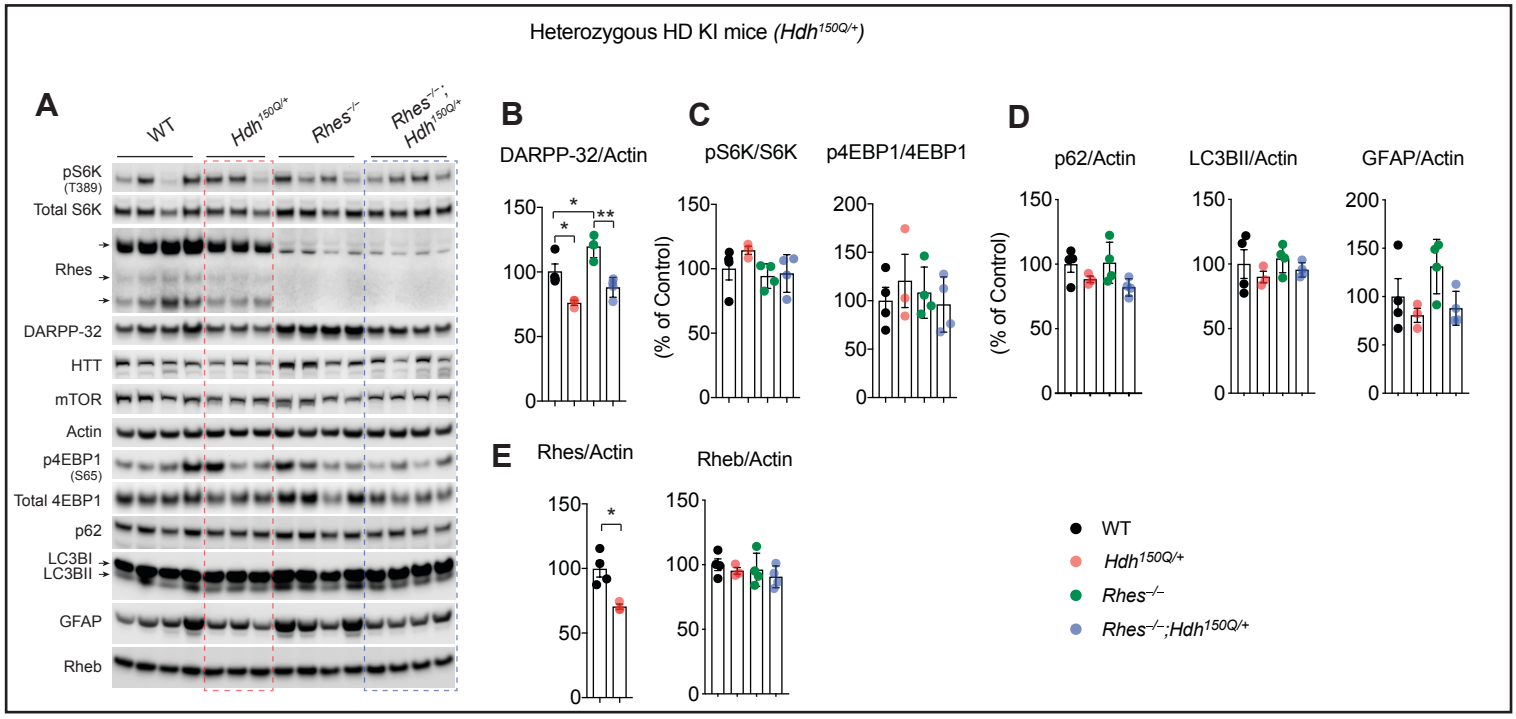

Figure 3